Formation of mega-scale glacial lineations far inland beneath the onset of the Northeast Greenland Ice Stream

Charlotte M. Carter[1,2], Steven Franke[3], Daniela Jansen[1], Chris R. Stokes[4], Veit Helm[1], John Paden[5], Olaf Eisen[1,2]

[1]Alfred-Wegener-Institut Helmholtz-Zentrum für Polar- und Meeresforschung, Bremerhaven, Germany
[2]Faculty of Geosciences, Universität Bremen, Bremen, Germany
5 [3]Department of Geosciences, Tübingen University, Tübingen, Germany
[4]Department of Geography, Durham University, Durham, United Kingdom
[5]Center for Remote Sensing and Integrated Systems, University of Kansas, Kansas, United States of America

Correspondence to: Charlotte M. Carter (charlotte.carter@awi.de)

Abstract. Rapidly-flowing ice streams drain the interior of the Greenland Ice Sheet, currently accounting for around half of
10 its annual mass loss. The Northeast Greenland Ice Stream (NEGIS) is one of the largest, recognisable almost 600 km inland,
and extends close to the central ice divide. Numerical ice sheet models are unable to accurately reproduce the configuration of
the NEGIS, but understanding its bed properties and spatial and temporal evolution is critical to predicting its future
contribution to sea-level change. Here, we use swath radar imaging to create a high-resolution Digital Elevation Model of the
bed close to where the NEGIS initiates. Surprisingly, this reveals a landscape interpreted to include mega-scale glacial
15 lineations (MSGLs) that are often assumed to be indicative of rapid ice stream flow (100s m yr^{-1}), under present-day flow
velocities of only ~60 m yr^{-1}. Given that MSGLs are thought to form under much higher flow velocities, their presence so far
inland at an onset zone raises important questions about their formation and preservation under ice streams, as well as past
configurations of the NEGIS. Elongate bedrock landforms outside the current shear margins also suggest that the NEGIS was
wider than its present configuration at some point in the past.

20 **1 Introduction**

The Greenland Ice Sheet (GrIS) is currently the largest contributor to global mean sea level rise from the polar ice sheets
(Otosaka et al., 2023). Its mass loss has increased sixfold over the last 40 years (Mouginot et al., 2019), around 50% of which
is accounted for by dynamic discharge via ice streams (Shepherd et al., 2020). One of the most prominent is the Northeast
Greenland Ice Stream (NEGIS), a 600 km long feature draining ~17% of the GrIS (Krieger et al., 2019) via fast-flowing
25 marine-terminating glaciers (Fig. 1a). The ice stream is characterised by several tributaries, the longest of which sharply
narrows as it extends inland towards the central ice divide, and is also unusual in that there is no obvious topographic steering
(Holschuh et al., 2019; Franke et al., 2020), meaning that the onset is not contained within a valley. The onsets of other ice
streams in Greenland that are topographically unconstrained, such as Petermann Glacier (Chu et al., 2018), are often much
wider and exhibit convergent flow into a main trunk, and lack such clearly defined shear margins, making the NEGIS unique
30 in its geometry. Rather, the origins of the NEGIS have previously been attributed to subglacial water produced by exceptionally
high geothermal heat fluxes in its onset zone (Fahnestock et al., 2001; Rysgaard et al., 2018; Smith-Johnsen et al., 2020),

although this is disputed (Bons et al., 2021). Despite its importance, numerical ice sheet models are unable to fully replicate the NEGIS's unusual flow configuration (Aschwanden et al., 2016). This discrepancy between numerical ice sheet models and modern-day ice flow velocities is thought to be partly due to the missing parameter of ice crystallographic preferred orientation

35   within the models (Gerber et al., 2023; Stoll et al., 2024), which can have an effect on the inferred basal drag or friction coefficient (Rathmann and Lilien, 2022), but may also be related to the representation of basal conditions.

Whilst the modern flow configuration and surface velocity of the ice stream is well constrained by satellite observations (Joughin et al., 2018) (Fig. 1a), much less is known about the bed properties and the spatial and temporal evolution of the NEGIS, the understanding of which is crucial to elucidating the driving factors which influence the ice stream. Basal properties

40   of the onset of the NEGIS have been constrained using single seismic lines, which were used to infer the, at least local, presence of saturated, high-porosity, deformable subglacial sediment (Christianson et al., 2014; Riverman et al., 2019). The presence of a streamlined bed, with potential elongate subglacial landforms in the upper reaches of the NEGIS, has also been hinted at indirectly via off-nadir reflections from widely spaced radar lines (Franke et al., 2020). In terms of the evolution of the ice stream, a recent study has revealed that the shear margins and flow configuration in the onset zone of NEGIS were only

45   established from around 2000 years ago (Jansen et al., 2024), questioning the assumption that the ice stream configuration had been stable throughout the Holocene (Fahnestock et al., 2001). Here, the amplitudes of folded internal reflection horizons from radio-echo sounding data indicate a record of the deformation of the ice stream, where the shear strain rates localised in narrow shear margins in the upstream part of the NEGIS ~2000 years ago (Jansen et al., 2024). Indeed, evidence from internal stratigraphy has also shown rapid reconfigurations in ice flow trajectories and drainage basin areas in northeast Greenland over

50   short (centennial) timescales during the Holocene (Franke et al., 2022a).
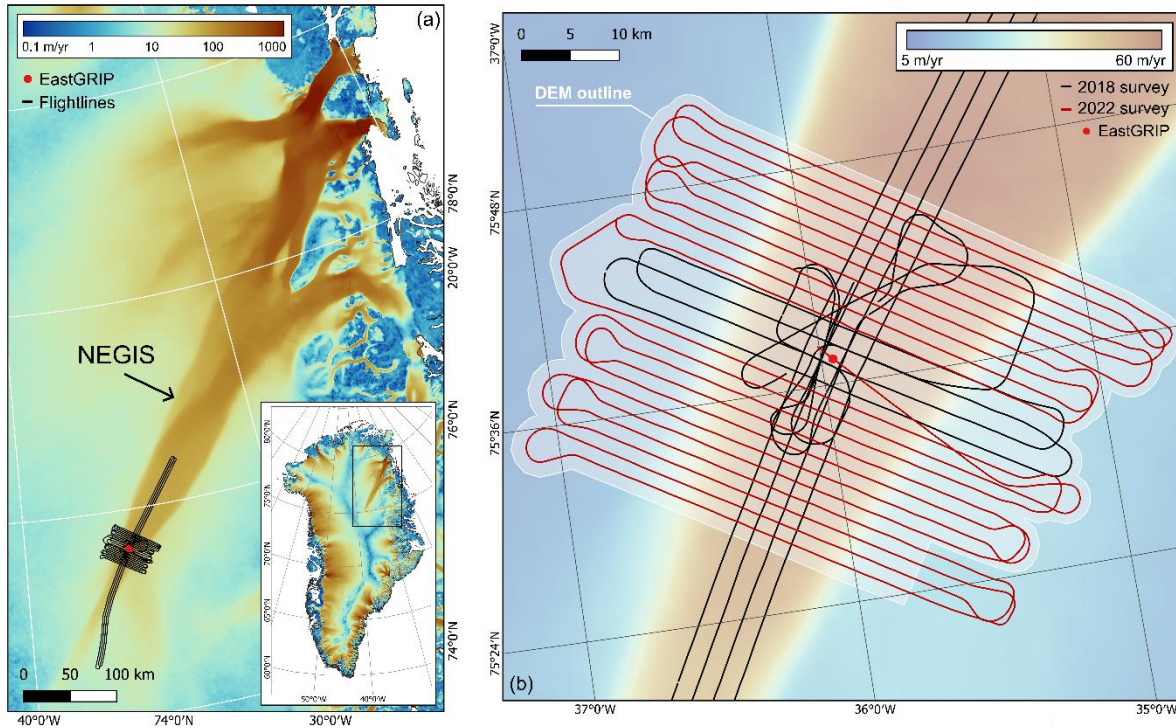
Figure 1: Overview of the study site in northeast Greenland. (a) NEGIS ice flow velocity (Gardner et al., 2022) with survey flightlines centred over the EastGRIP ice core site (red dot). Inset map shows ice flow velocity across Greenland on a logarithmic colour scale. (b) Survey flightlines in swath mode at the onset of NEGIS with an outline (light grey) of
55 **the generated DEM, and ice flow velocity in the background.**

In order to further investigate the basal properties that lie beneath the onset of the NEGIS, this paper presents the first high resolution (25 m horizontal resolution, ~10 m vertical resolution) Digital Elevation Model (DEM) of the subglacial topography, reconstructed from swath radar, which is capable of identifying individual subglacial bedforms. The DEM covers a 40 x 60 km^2 area surrounding the EastGRIP ice core site (Fig. 1b), where the ice thickness reaches 2.5 km and ice flow velocities are

60 around 60 m yr^{-1}. Previously mapping of *in situ* subglacial bedforms under other active ice streams at such a high resolution has been achieved with conventional nadir-focused radar techniques, which derive bed elevation from closely-spaced radar lines and use interpolation (King et al., 2016; Bingham et al., 2017; Schlegel et al., 2022). These methods, whilst providing excellent observations, have an inherent limitation in their cross-track resolution and spatial coverage, in that direct point measurements of the bed are only possible in the along-track direction. Instead, with swath radar processing, there is no

65 requirement to interpolate between these point measurements, as the direction of the arrival of energy in both the along-track and across-track directions can be estimated from the sequential acquisitions. Therefore, the topography can be reconstructed

in high resolution over kilometre-wide strips, and the imaging of subglacial bedforms is possible at a lower logistical cost (Holschuh et al., 2020) and over a much wider spatial area.

Importantly, swath radar data surveys enable a view into the small-scale subglacial topography and landforms that reside beneath active ice sheets. This has a range of advantages, from identifying geomorphological features, to enabling the incorporation of small-scale variations in basal topography within ice flow models, which can produce modelled ice motion patterns that diverge substantially from those utilising smoothly varying topography (Law et al., 2023). Two other similar surveys of swath radar data have been generated in Antarctica (Holschuh et al., 2020; Hoffman et al., 2023), which investigate the subglacial geomorphology beneath Thwaites Glacier and Hercules Dome. These data, alongside our DEM, provide crucial insight into the formation of subglacial landforms, which previously have only been accessible and studied within the context of deglaciated landscapes. For example, when elongate subglacial landforms are identified on a deglaciated landscape, they are utilised as a proxy to reconstruct previous ice sheet extent and dynamics (Margold et al., 2015; Stokes et al., 2015). Mega-scale glacial lineations (MSGLs), for example, are generally associated with high flow velocities under ice streams (King et al., 2009; Stokes et al., 2013; Spagnolo et al., 2014). In addition, the elongation of these landforms has often been said to follow a down-flow morphological continuum, where they evolve from flow-perpendicular landforms at the onset (for example, ribbed moraines) to elongated flow-parallel MSGLs, as a product of increasing ice flow velocity and changing basal conditions, such as cumulative strain at the bed (Ely et al., 2016; Zoet et al., 2021; Vérité et al., 2023). However, the inferred link between MSGLs and fast ice streaming is largely qualitative with very few quantitative modelling studies (Jamieson et al., 2016; Ely et al., 2022), and there is little consensus around their mechanism of formation (Spagnolo et al., 2014; Stokes, 2018).

The data presented here comprise the first high-resolution subglacial topography survey beneath the onset of an ice stream in the deep interior of the GrIS, located around 600 km from the grounding line. The classification of the now visible geomorphological features provides insight into both the basal conditions of the ice stream and its evolution. The identification of MSGLs beneath the onset also raises important questions around their formation and preservation beneath ice streams, given the relatively low ice flow velocities.

2 Methods

2.1 Generation of swath data

The Alfred Wegener Institute's ultra-wideband radar system (AWI-UWB) (Hale et al., 2016; Franke et al., 2022b) was used to map the cross-track topography at a horizontal resolution of 25 m, in swaths ~2 km wide (Fig. 2). The majority of the flightlines were oriented perpendicular to the direction of ice flow, in order to reduce the possibility of artefacts that could be misinterpreted as flow-parallel subglacial landforms (Fig. 1b). Historically, the ability to resolve the detail of subglacial

topography from airborne radar surveys has been dictated by along-track spacing, survey line spacing and along-track focusing, as conventional bistatic antenna airborne radar is unable to localise energy in the cross-track direction. Therefore, to produce a high-resolution digital elevation model of the bed, we apply swath processing techniques to ultra-wideband radar data
100 collected by the AWI-UWB radar system in 2018 and 2022, surrounding the EGRIP ice core site. Using a multi-element antenna array (Fig. 2a) means that information from sequential acquisitions, combined with phase differences in arrivals between receiver elements (Holschuh et al., 2020; Jezek et al., 2011), can be used to estimate the direction of arrival for energy in both the along-track and across-track directions (Paden et al., 2010) (Fig. 2b). Application of the Multiple Signal Classification (MUSIC) algorithm in the Open Polar Radar toolbox (Paden et al., 2023) to SAR-processed radar data therefore
105 allows mapping of the subglacial topography in three dimensions along a single flight line.
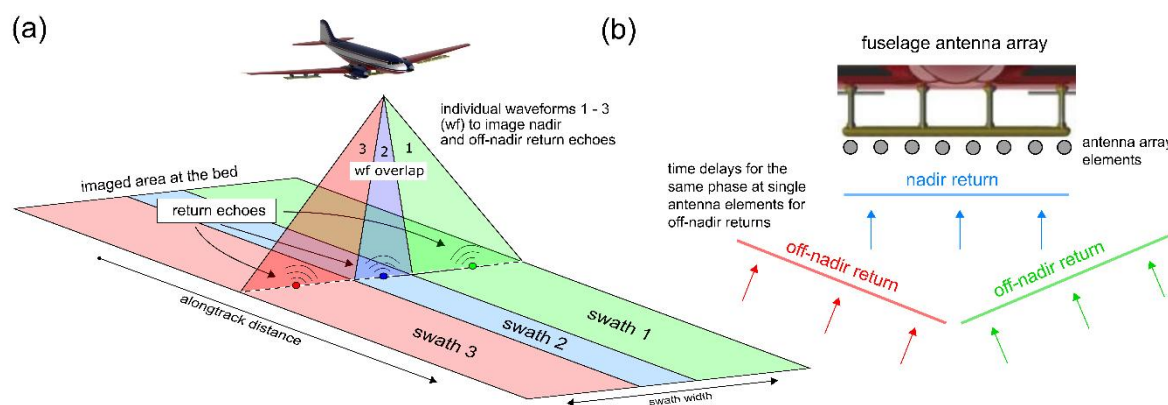
Figure 2: (a) Individual waveforms from a multi-antenna radar array used to image both nadir and off-nadir return echoes from the ice-bed interface. (b) Time delays for the same phase at single antenna elements are used to geolocate the off-nadir return echoes.

110 Along-track and fast-time averaging was applied to the SAR-processed data to improve the signal-to-noise ratio when tracking the bed return and cross-track surface. In the along-track direction, the depth range where the bed return was expected was selected using bed elevation values from BedMachine v.5 (Morlighem et al., 2017; Morlighem et al., 2022). The nadir bed return is picked in order to produce seed points from which the cross-track reflector is digitised, to geolocate off-nadir reflection information (Al-Ibadi et al., 2017). In the cross-track surface picking (Fig. 3a), the bed return power was fitted to a gaussian
115 distribution in order to overcome the broad distribution and multiple peak bed returns from which the maximum is picked. Tracking of the bed pick is limited using a guided window based on a theoretical hyperbola of a flat bed, as there are often englacial reflections close to the bed return. A -2.5° static angle correction was also applied to account for tilting in the tracked cross-track surface. For each trace, after cross-track surface tracking, the hyperbola of the bed return is range migrated, including the refraction of air to ice, to convert the surface tracking to depth (Fig. 3b). Here, upwarping at the edges of each

120   swath introduced some artefacts into the data, as spreading of the bed return energy reduced the accuracy of the surface
       tracking. Whilst this could have been excluded from the final DEM, reducing the swath width prevented overlap of each swath,
       meaning that landforms could not be mapped distinctly. The range migrated data produced a point cloud, which is projected
       from the reference frame to geographic coordinates (latitude and longitude) using the true heading and flight trajectory from
       the radar data. The final DEM raster is then interpolated from the georeferenced point cloud dataset using inverse distance

125   weighting, at a pixel spacing resolution of 25 m and a vertical resolution of ~10 m. The resulting product is a three-dimensional
       tomographic image of the ice base, with swath widths of ~2 km.
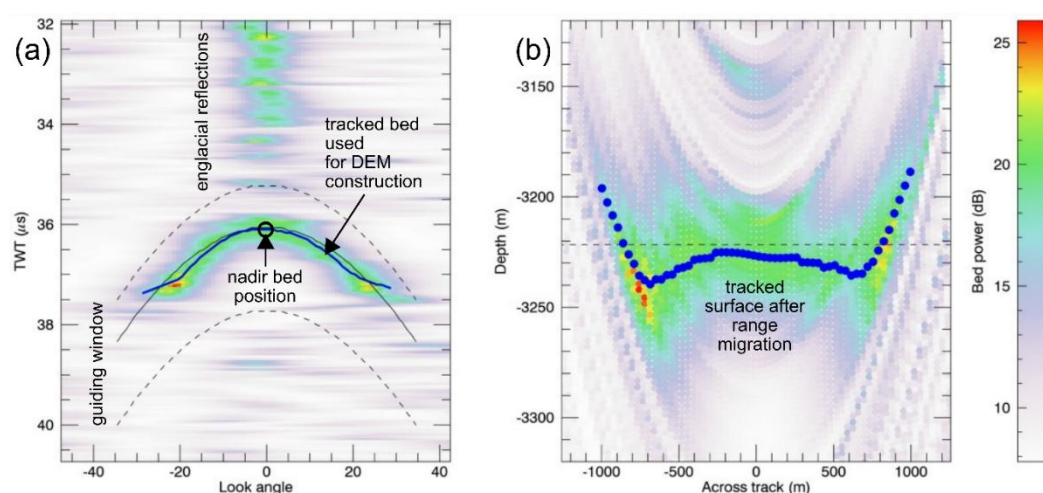
Figure 3: (a) Cross-track surface tracking at each nadir bed position produced from the MUSIC algorithm (Paden et al., 2010). (b) The tracked surface is range migrated to convert the two-way travel time values to depth.

130   **2.2 Characterisation of the subglacial landscape**

       In order to characterise the subglacial landscape, digital geomorphological mapping of the landforms was carried out in QGIS
       v3.26.3 (Qgis.Org, 2025) (Fig. 4). Multiple hillshade directions and contour lines were utilised to define the edges of landforms
       (Chandler et al., 2018), which were manually delineated across the DEM. The landforms were initially categorised, without
       interpretational bias, as geomorphic ridges, lineations, channels, and basins. Lineations, interpreted as MGSLs, (Fig. 4a) were

135   identified as linear, low relief, and flow-parallel features, which generally have elongation ratios greater than 10:1, and are
       consistent in terms of width (Stokes and Clark, 2002a; Stokes et al., 2013; Ely et al., 2016). Geomorphic ridges, in contrast to
       lineations, are landforms that are less consistent in their width and less elongate, meaning that they were more circular or
       irregularly shaped. These geomorphic ridges were interpreted as three different categories: crag-and-tails (Fig. 4b), Barchan
       drumlins (Fig. 4c), or a shear margin moraine (Fig. 4f). Crag-and-tails can be identified as streamlined bedrock outcrops or

140   ridges, with a steep stoss side and tapering lee side tail that is usually composed of unconsolidated sediment (Dowdeswell et

al., 2016; Nitsche et al., 2016). Barchan, or erosional, drumlins are identified as bedrock ridges that are dissected into smaller outcrops, grouped in a crescentic shape (Eyles et al., 2016). The potential shear margin moraine was identified as it is a long, low relief, narrow feature aligned with the shear margin, but clearly misaligned with ice flow direction and the flow-parallel MSGLs (Stokes and Clark, 2002b). Channels are incised valleys that cut across the landscape as linear depressions (Fig. 4e).

145 These channels curve around a topographic high point, and could be interpreted as meltwater channels, or potentially tunnel valleys, which are defined by their kilometre-scale widths and undulating thalwegs, which indicates incision by subglacial meltwater (Kehew et al., 2012; Livingstone and Clark, 2016). Basins were mapped as flatter areas in topographic low points (Fig. 4d), often between larger ridges, and are likely to contain sediments due to their smoother appearance as compared to the areas of bedrock outcrops (Roberts et al., 2019; Dowdeswell et al., 2016).

150 Elongation ratios were calculated in QGIS as the length of a minimum bounding rectangle divided by the width. As the swath processing introduced some artefacts into the DEM, due to upwarping at the edge of each swath creating flow-perpendicular rises in elevation, only landforms which are clearly identifiable as geomorphological features, and could definitively be observed crossing multiple swath widths, were mapped.
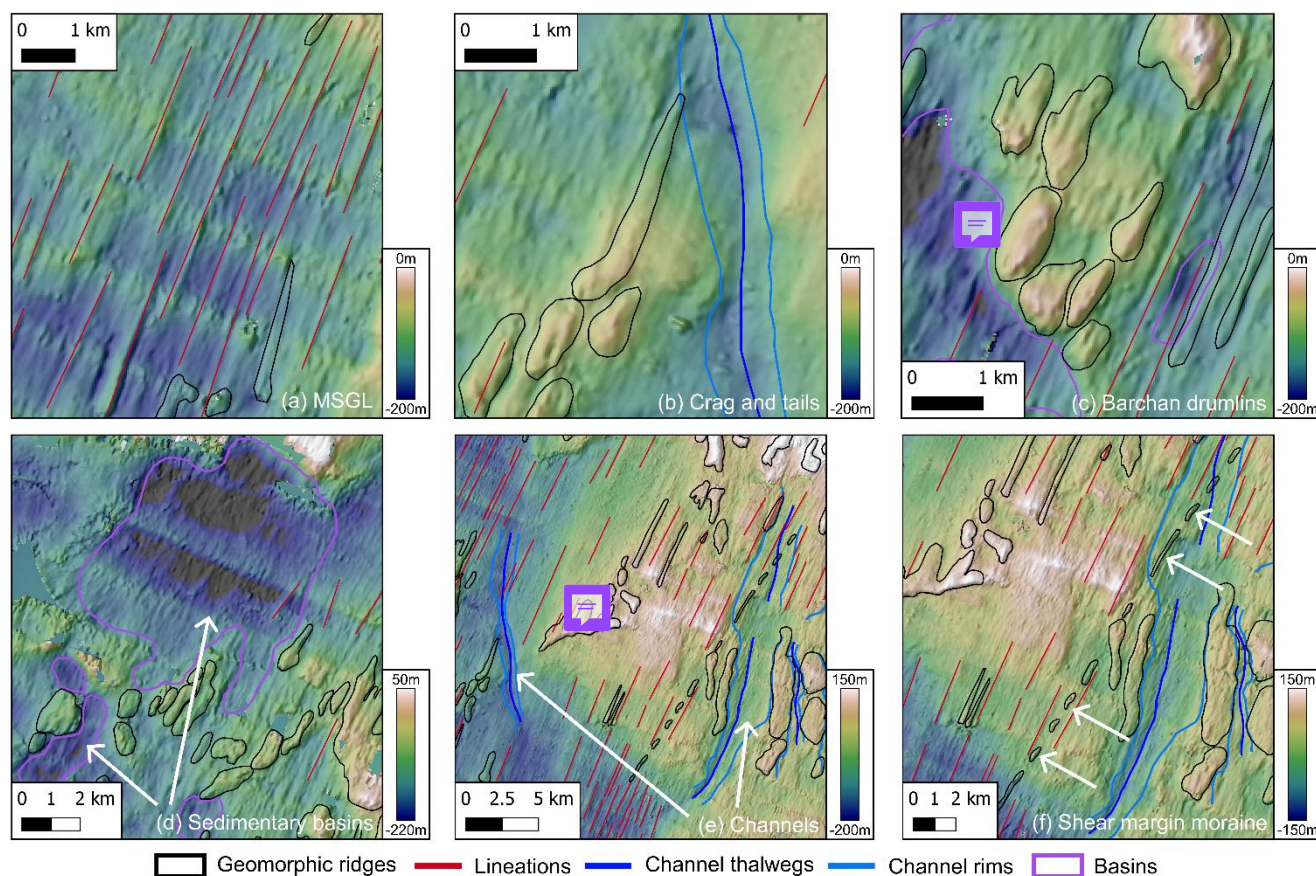
155 **Figure 4: Examples of subglacial landforms identified beneath the onset of the NEGIS. The initial non-interpretational mapping of lineations (red lines), geomorphic ridges (black outlines), channels (dark blue thalwegs, light blue rims) and basins (purple outlines) is shown in each panel. These landforms were then interpreted as described above, examples of which are shown in each panel: (a) Mega-scale glacial lineations. (b) Crag and tails. (c) Barchan/erosional drumlins. (d) Sedimentary basins. (e) Meltwater channels. (f) Shear margin moraine.**

160 **2.3 Comparison of landforms to velocity data and shear margins**

The NASA MEaSURES ITS_LIVE velocity mosaic (Gardner et al., 2022) was used to derive the streamlines of the current velocity field, as well as the overlying surface velocity related to each landform. The mean velocity value within each polygon was used as a representative value for each individual landform. The shear margins of the ice stream were delineated where the shear strain rate was at its maximum value from multiple cross-profiles. The shear strain rate was derived from TerraSAR-

165 X ice velocity data (Hvidberg et al., 2020). Relative locations of subglacial landforms within or outside of the shear margins were determined using the outermost shear margin where the shear margins overlap, and the polygon delineating the landform had to be contained entirely within the shear margin boundaries.

3 Results

3.1 High resolution subglacial geomorphology at the onset of the NEGIS

170 A detailed image of the subglacial landscape is shown in Fig. 5, with our mapping of the landform assemblage shown in Fig. 6a (see also Fig. 4). Low relief, highly elongated lineations are interpreted as MSGLs (Fig. 4a) and are almost entirely constrained within the modern shear margins of the NEGIS (Fig. 5). The elongation ratios of these lineations range between 7.7:1 and 59.2:1, with the more elongate features generally located beneath the central trunk of the NEGIS (Fig. 6b). The majority are oriented in the direction of the overlying surface flow, although some close to the shear margins are oriented at

175 an angle up to 13° away from the trajectory of the current flow field. Heights of the MSGLs have a mean value of 66.5 m, and range between 21 m (minimum) and 148.4 m (maximum). The MSGLs range from 968 to 7397 m in length, with a mean value of 3025 m (Fig. 6c), but some are truncated by bedrock ridges that have a rougher appearance in the landscape. In addition, there are instances where the bedrock ridges appear to act as seed-points for the MSGLs, which then continue downstream into the sedimentary basins and have a much smoother appearance (see identified MSGLs in Fig. 5).
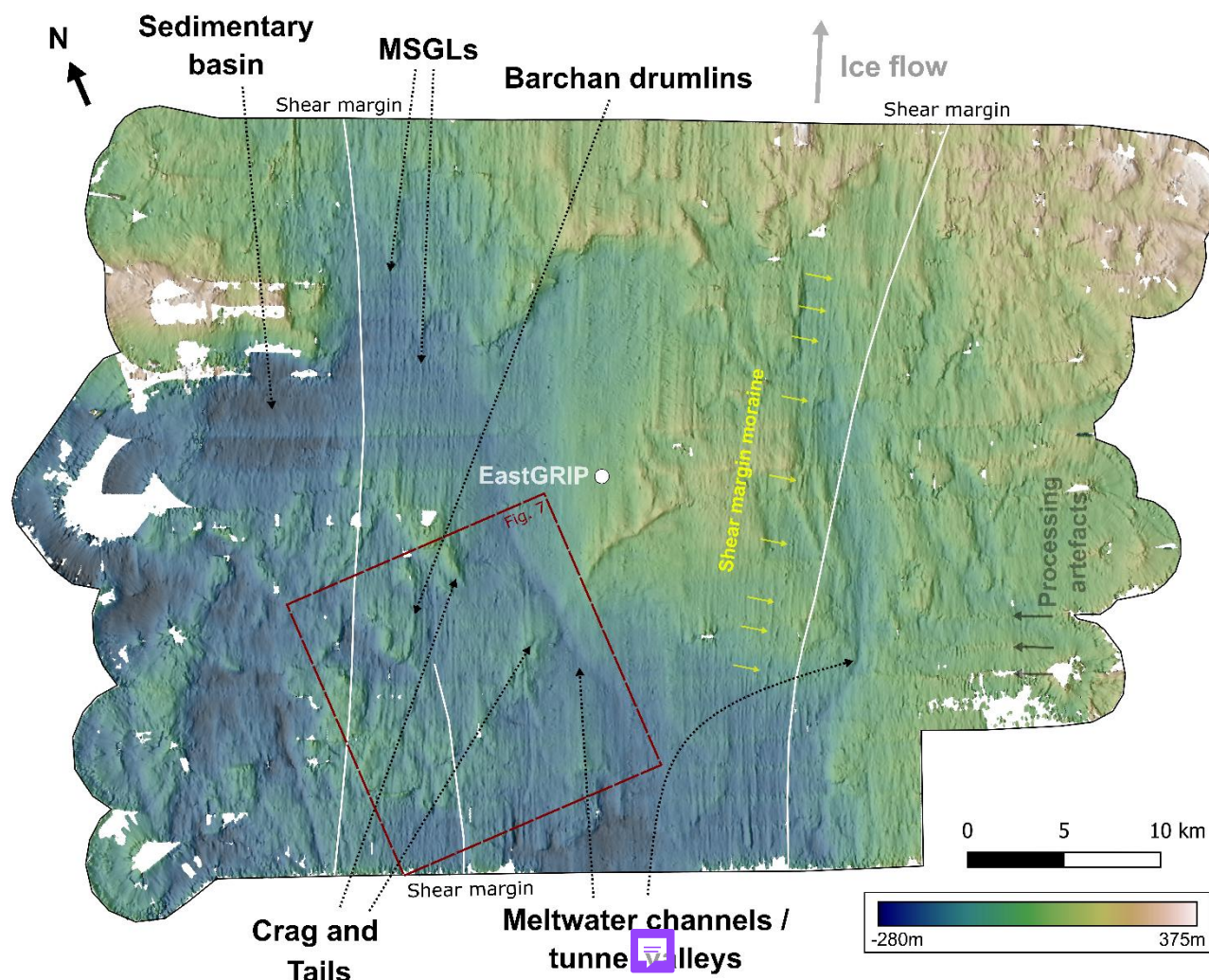
Figure 5: Subglacial topography produced from swath radar measurements at the onset of NEGIS. The hill-shaded DEM (referenced to WGS84) allows interpretation of an assemblage of subglacial landforms, characteristic of ice streaming, such as mega-scale glacial lineations, crag and tails, and barchan drumlins. Location of the survey shown in Fig. 1 and the red box shows the location of Fig. 7. Arrows on top indicate True North and direction of ice flow.

185   The mapped geomorphic ridges are interpreted as mainly bedrock features, mostly resembling crag and tails (Fig. 4b, metrics in Table A1). These are elongate features with a steep stoss side on the outcrop and lee side tails oriented in the direction of overlying ice flow. They are differentiated from MSGLs by their higher relief and with stoss-side outcrops having a rougher appearance, with a smoother tapering lee-side tail. There are some potential barchan, or erosional, drumlins (*sensu* Eyles et al. (2016)), which are identified based on the grooves carved into the bedrock ridges, bisecting a larger 'parent' drumlin into

190   smaller outcrops that are grouped together in a crescentic shape (Fig. 4c). The bedrock ridges are clustered in groups, particularly in the southwest of the survey area, and are present both within and outside of modern shear margins, more evidently on the western side. The distribution of elongation ratios of these ridges demonstrates that they show some degree of elongation outside of the shear margins, as well as inside (Fig. 6d).

Other features include depressions within which are likely to be softer/unconsolidated sediments, rather than hard bedrock, as
195   might be suggested by their smoother appearance, and previous seismic surveys indicating the presence of saturated subglacial sediment in this region (Christianson et al., 2014). These sediments contained within the basins (Fig. 4d) appear as flatter areas in topographic lows, which are often downstream of bedrock features, the largest of which has an area of 49 km^2. Some large (between 0.5 - 3 km wide) incised channels are also identified, often deviating around topographic highs and cutting across the landscape both inside and outside of the ice stream (Fig. 4e). These are interpreted as large meltwater channels, and
200   potentially tunnel valleys (Livingstone and Clark, 2016; Kehew et al., 2012), although the possibility remains that they are part of a preserved fluvial network.

A long narrow feature aligned closely with the south-eastern shear margin (see yellow arrows in Fig. 5) is interpreted as a lateral shear margin moraine (Stokes and Clark, 2002b), based on its proximity and alignment with the shear margin, its continuity across multiple swaths, and its relief of between 30 to 40 m that is prominent in the surrounding landscape (Fig. 4f).
205   The ridge appears to be dissected in places, but this is likely due to artefacts at the edge of each overlapping swath (see Methods and Fig. 3a).
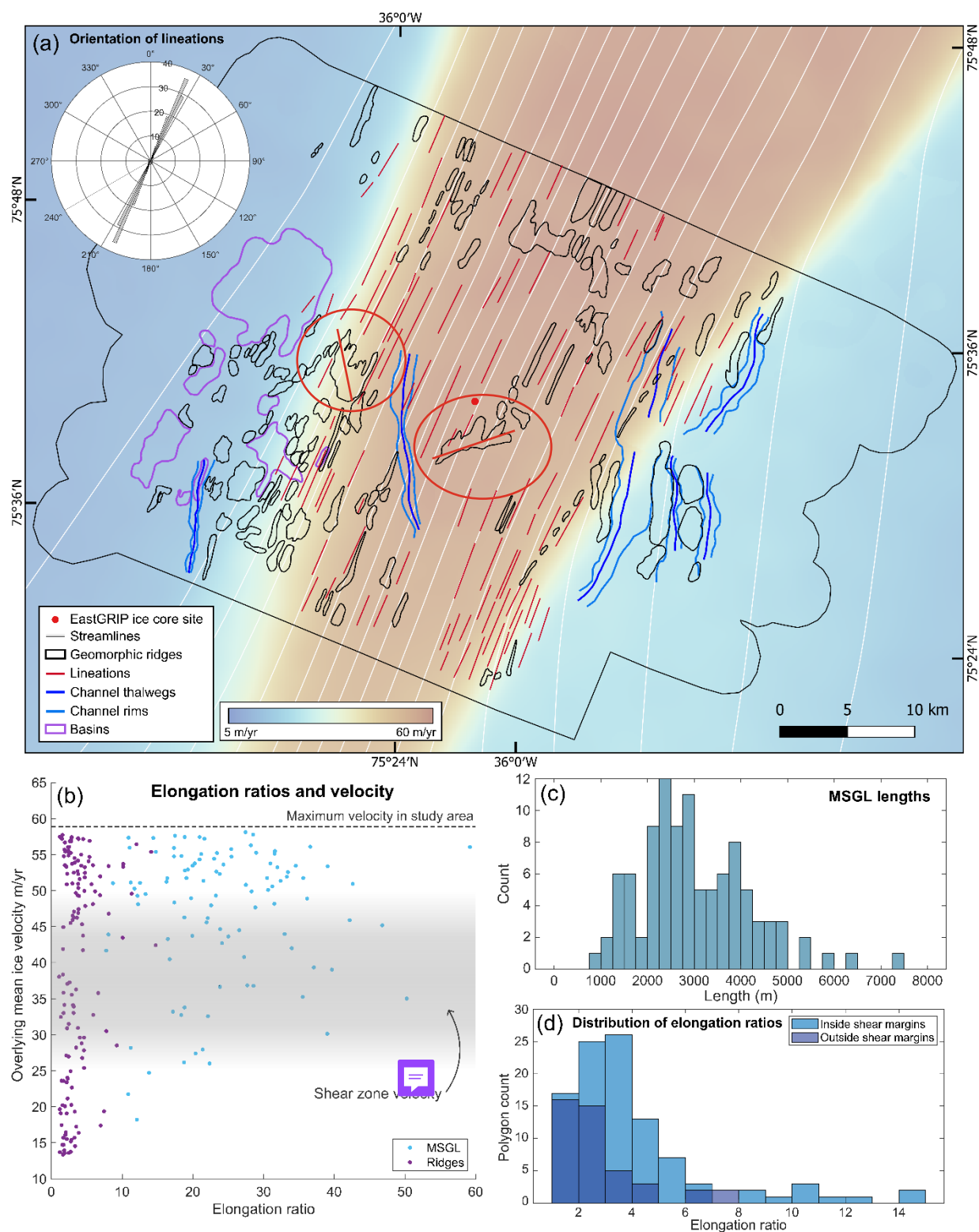
Figure 6: Subglacial landform mapping related to the overlying ice dynamics. (a) Geomorphological mapping of the subglacial topography, with surface ice flow velocity (Gardner et al., 2022) and streamlines (Hvidberg et al., 2020), which are flow-parallel lines, illustrating the direction of flow of the current steady-state velocity field. Inset polar histogram shows the orientation distribution of the MSGLs. (b) Scatter plot showing the elongation ratios of the MSGLs and geomorphic ridges compared to surface flow velocity. (c) Histogram of MSGL length. (d) Histogram of the elongation ratios of the geomorphic ridges, both within and outside of the modern shear margins of NEGIS.

4 Discussion

4.1 Implications for the basal conditions and spatial evolution of the NEGIS

Classification of the geomorphology beneath the onset of the NEGIS allows us to infer some aspects of the basal properties, as the differing regions of subglacial landforms would suggest heterogeneity of the bed. The geomorphology bears close resemblance to a 'mixed bed' landform assemblage (Fig. 7), composed of a combination of hard bedrock outcrops interspersed with softer sediments and subglacial bedforms, such as those identified on palaeo-ice stream beds in west Greenland (Dowdeswell et al., 2014), the Amundsen Sea Embayment (Graham et al., 2009) and the North Sea (Roberts et al., 2019) (Fig. 7). These types of subglacial landscapes are characterised by the presence of crag and tails, drumlins, and highly elongate lineations, and thought to be formed under ice streams (Roberts et al., 2019; Dowdeswell et al., 2014; Graham et al., 2009). Previous seismic data from around the EastGRIP ice core site (Christianson et al., 2014) inferred saturated, high-porosity, presumably deforming sediment within the main trunk of the ice stream, and non-deforming and more compacted sediments outside of the main trunk. However, the presence of crag-and-tails would imply additional bedrock outcrops in the broader region of the onset now visualised by our new DEM. The observations from Christianson et al. (2014) led to the hypothesis that an underlying layer of dilatant till might explain the inception of the ice stream in this location and its lack of a major subglacial trough, but our observations of a mixed bed landform assemblage, and the presence of large discrete meltwater channels, would suggest that the characteristics of the bed are perhaps more heterogenous than previously recognised.
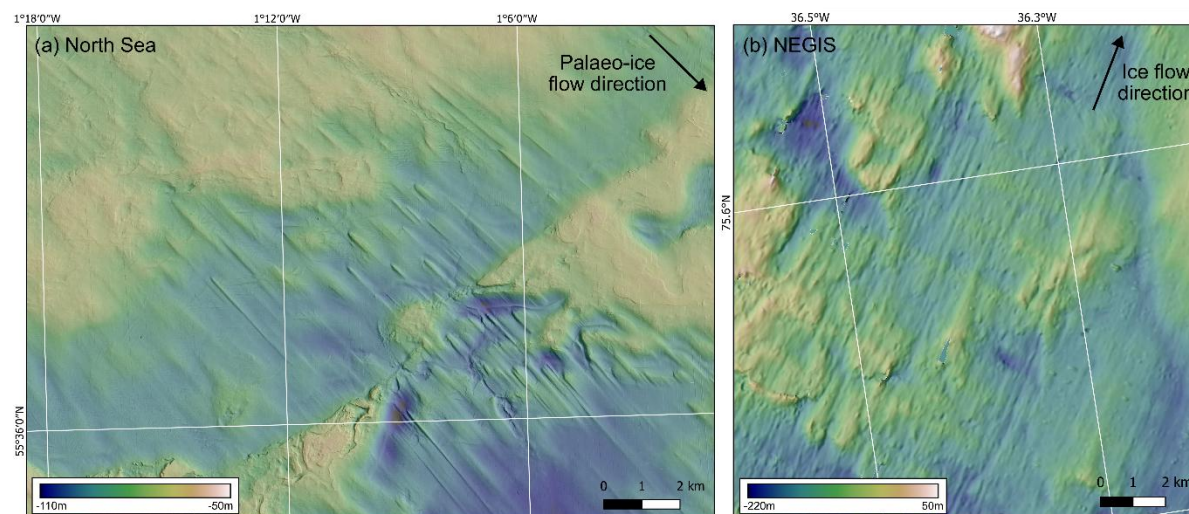
Figure 7: Comparison of mixed-bed landform assemblages. (a) North Sea bathymetry data showing streamlined bedforms and bedrock highs (Roberts et al., 2019). (b) Bedrock features beneath the onset of NEGIS (inset in Fig. 5).

Within this mixed-bed assemblage, the distribution of the identified subglacial landforms can be used to infer changes in the location of the ice stream shear margins, using the crag-and-tails, which are commonly used as indicators of fast palaeo-ice flow (Nitsche et al., 2016; Dowdeswell et al., 2010; Dowdeswell et al., 2016). The degree of elongation of crag-and-tails outside the present shear margin is similar to those inside of the shear margins (Fig. 6c, Table A1), indicating a potential spatial evolution of the shear margins of the NEGIS. It suggests that they could have been subject to similar flow conditions as inside the shear margins of the current ice stream at some point in the past, as the current overlying ice velocity conditions outside of the shear margins are slower, and not streaming (10 to 25 m yr^{-1}, Fig. 6b). The crag-and-tails are more prevalent on the north-western side of the ice stream compared to the southeast, which correlates with internal folding of ice horizons that demonstrate a 'jump' between an active and inactive section of the north-western shear margin, where the margin has shifted inwards (Jansen et al., 2024). The south-eastern shear margin, however, has a much more abrupt transition between the slow-flowing and fast-flowing ice inside of the ice stream trunk. The transitory nature of the north-western shear margin could, therefore, be related to a potential narrowing of the ice stream associated with the localisation of the shear margins, as streaming conditions would have overlain the ridges currently outside of the shear margins. Therefore, we propose that the ice stream may have been up to 10 km wider at some point in the past, or experienced convergent or a slightly different direction of flow prior to the localisation of the current shear margins (Bons et al., 2016; Jansen et al., 2024). The relative lack of elongate ridges, as well as the preservation of a potential shear margin moraine evident along the south-eastern shear margin, suggest a more stable configuration on this side.

4.2 Implications for MSGL formation

Subglacial landforms used to reconstruct palaeo-ice streams, such as drumlins and MSGLs, have often been argued to represent a subglacial morphological continuum that evolves with cumulative basal slip speed (Stokes et al., 2013; Ely et al., 2016; Barchyn et al., 2016; Zoet et al., 2021; Ely et al., 2022; Vérité et al., 2023). Along this continuum, ice flowing at velocities of 10s to <100 m yr^{-1}, i.e. similar to the velocity at the onset of NEGIS, has typically been associated with landforms oriented perpendicular to ice flow direction known as ribbed moraines, but merging into classic drumlins as velocity increases (Stokes et al., 2013). Hence, ice stream onset zones are thought to be associated with landforms that are transverse to ice flow, or oriented in the direction of ice flow but with low elongation ratios that are more characteristic of drumlins, rather than MSGLs (Anderson and Fretwell, 2008; De Angelis and Kleman, 2008; King et al., 2009). As ice velocities increase to 100s m yr^{-1}, drumlins have been hypothesised to evolve and elongate into MSGLs (Stokes et al., 2013; Barchyn et al., 2016; Ely et al., 2022).

The geomorphological signature beneath the onset of NEGIS has a clear ice streaming imprint with the presence of MSGLs, which is perhaps surprising given that ice velocities within the study area currently peak at 58 m yr^{-1}. All previous observations of MSGLs beneath active ice streams are associated with ice velocities >100 m yr^{-1}, such as the landforms detected beneath the main trunks of Rutford Ice Stream (Schlegel et al., 2022) (380 m yr^{-1}) and Thwaites Glacier (Holschuh et al., 2020) (between 100 and 400 m yr^{-1}), which have formed under continuous and relatively stable high-velocity ice streaming conditions (Alley et al., 2021; Woodward and King, 2009; Gudmundsson and Jenkins, 2017). The setting of these ice streams contrast with the much more variable nature (Franke et al., 2022a) and slower (< 60 m yr^{-1}) velocities at the onset of the NEGIS. To our knowledge, the only other high-resolution survey of an ice stream onset zone (King et al., 2007) revealed classic drumlin forms (elongation ratios 1:1.5 to 1:4) and a potential ribbed moraine under Rutford Ice Stream, West Antarctica, where velocities accelerate from 72 to >200 m yr^{-1}. Furthermore, the location of the MSGLs in our study, 600 km from the grounding line and only ~200 km from the main ice divide, is also the furthest inland that MSGLs have been identified.

There are a number of hypotheses that might explain the presence of MSGLs beneath the modern-day slow ice velocities observed at the onset of the NEGIS. Firstly, it could be argued that a plausible hypothesis to explain the presence of the MSGLs under this part of the NEGIS, is that the study area experienced higher ice velocities in the past, after which the MSGLs have simply been preserved. This might therefore suggest that ice velocities under this part of the NEGIS were much higher (>100 m yr^{-1}) at some point in the past. However, it is unlikely that the NEGIS experienced higher ice velocities prior to the localisation of the shear margins 2000 years ago, as the advection of the folding of the internal stratigraphy, in conjunction with the shear strain rates present within the shear margins, would suggest a previous confluent flow regime with similar or lower velocities than present (Jansen et al., 2024). When the shear margins localised in their current location, the ice stream was decoupled from the interior of the ice sheet, which, at that point in time, enabled the faster flow observed at present. Higher velocities would have produced higher shear strain within the margins, which has not been observed. Modelling of the ice

stream dynamics of the northeastern sector of the Greenland Ice Sheet since the Last Glacial Maximum has also shown no indication of higher velocities within the interior of the ice sheet, prior to the formation of the NEGIS (Tabone et al., 2024). Thus, we would consider the plausibility of these MSGLs being formed from a faster configuration of the NEGIS to be unlikely.

Secondly, it could be argued that the MSGLs under the onset of the NEGIS were formed by the current slow ice velocities over much longer (multi-millennial) timescales (Clark, 1993), where the present NEGIS has been very stable in this location at this flow speed. However, it has been shown that the NEGIS is a relatively young ice stream and that this sector of Greenland has undergone drainage basin reconfiguration over the Holocene (Franke et al., 2022a; Jansen et al., 2024). Earlier configurations of now-extinct ice streaming in the northeastern part of the ice sheet during the Holocene did not reach so far into the interior (Tabone et al., 2024; Franke et al., 2022a), instead draining a more northerly part of the ice sheet, indicating that the NEGIS as seen today is a relatively recent feature established within the last 2000 years (Jansen et al., 2024). Thus, although we are unable to rule out that the MSGLs may have formed by slow flow over a much longer duration, we view this as unlikely because they correspond to the margins of the present enhanced flow, rather than everywhere across the study area. Indeed, if that were the case more generally, then MSGLs would be far more common on both palaeo and modern ice sheet beds.

A third possibility is that the MSGLs are more akin to bedrock mega-grooves and, therefore, their length is not directly related to ice velocity (Newton et al., 2018). However, we reject this hypothesis, as the morphometric characteristics of the MSGLs here are different to those relating to bedrock mega-grooves (Newton et al., 2023). The heights of the MSGLs average 66.5 m, which are much greater than the depths seen in bedrock mega-grooves (5 – 15 m (Newton et al., 2023)). Whilst some studies have shown the majority of amplitudes of MSGLs to have low heights (between 1-9 m, Spagnolo et al. (2014)), MSGLs of the scale identified here have also been observed beneath Thwaites Glacier, where elongated bedforms composed of soft till locally exceed 100 m in height (Alley et al., 2021), as well as in past ice streams off the Antarctic Peninsula (Canals et al., 2000). The contrast of the rougher bedrock outcrops to the smoother appearance of the MSGLs would also indicate that this is a mixed bed assemblage (Roberts et al., 2019), as the landscape is akin to a transitional 'mixed bed' zone, where streamlined bedrock features and MSGL occur adjacently as the subglacial bed changes between hard and soft material (Mulligan et al., 2019; Eyles and Doughty, 2016).

Whilst we cannot rule out an episode of enhanced flow at this location in a previous glaciation, the sedimentary basins outside of the northwestern shear margin (Fig. 6) show little evidence of MSGL formation. This would mean that the ice stream would have to have formed in the same configuration as observed today in a prior glaciation, potentially with a higher velocity, to produce the observed MSGLs. Even so, if this had occurred, this would then suggest that MSGLs can be preserved for 100s to 1000s of years under relatively slow ice velocities. Rather, we propose that these MSGLs within the current shear margins,

are likely to have formed in situ under modern-day slow ice velocities (<60 m yr^{-1}), over the 2000 years in which the NEGIS onset has existed at this location, questioning the paradigm that they are exclusively associated with fast ice flow.

5 Conclusions

In conclusion, high-resolution bed topography data from swath radar enables key observations into the basal conditions of an ice stream, as well as its potential spatial evolution. The identification of the previously unseen subglacial geomorphology beneath the onset of the NEGIS allows insight into the processes under which these landforms form. The presence of MSGLs so far inland under the NEGIS is a surprising discovery, given that ice velocities are < 60 m yr^{-1} and the study area is only ~200 km from the ice divide. We deem it unlikely that the MSGLs were formed by slow ice flow over a much longer duration than 2000 years, but are unable to rule out the possibility that a previous episode of fast flow created the MSGLs, which would have since been preserved under ice flow conditions similar to present. However, we view this as unlikely given that the folding of the internal stratigraphy and shear strain rates of the margins indicate a slower, confluent flow regime preceding the formation of the shear margins. Rather, our favoured interpretation is that the MSGLs are the product of the relatively low ice velocities (10s of m yr^{-1}) observed today, within the 2000-year timescale of the current configuration of the NEGIS. If correct, these observations may prompt a re-evaluation of some models of MSGL formation and their use as an indicator of high (>100s m yr^{-1}) ice velocities, but further work, such as a multitemporal analysis, is required to examine whether the features are relicts from a previous flow regime or are actively forming under current conditions.

Appendix A

		Geomorphic ridges	Geomorphic ridges (within shear margins)	Geomorphic ridges (outside of shear margins)
Sample size		144	101	43
Length	Min	409.5	558.3	409.5
	Max	7593.7	5860.1	7593.7
	Mean	2009.3	2004.2	2021.2
	Median	1680.9	1705.7	1533.3
	St. dev.	1230.3	1108.9	1491.8
Width	Min	203.5	203.5	223.6
	Max	3680.2	3680.2	2105.6
	Mean	663.2	619.8	764.9
	Median	562.8	505.6	708.6

	St. dev.	501.9	518.2	450.8
Elongation ratio	Min	1.1	1.1	1.2
	Max	14.7	14.7	7.7
	Mean	3.7	4.1	2.8
	Median	3.0	3.4	2.3
	St. dev.	2.5	2.7	1.7
Height	Min	27.0	28.0	27.0
	Max	212.3	212.3	199.2
	Mean	80.1	75.9	90.5
	Median	72.5	68.6	80.6
	St. dev.	37.1	35.0	40.2

330 **Table A1: Quantitative metrics of geomorphic ridges mapped.**

Data availability

The DEM raster GeoTiff constructed from AWI UWB swath mode RES data is available at PANGAEA (doi pending, temporary reviewer access key available). Multibeam echosounder bathymetric data from the North Sea (Fig. 7) was downloaded from the UK Hydrographic Office under the Civil Hydrography Programme
335 (https://data.admiralty.co.uk/portal/apps/sites/#/marine-data-portal).

Author contribution

OE, SF, and CMC conceptualised the study. DJ and JP collected the survey data, which was processed by VH, SF, and CMC, with the method being developed by VH. CMC prepared the manuscript with contributions from all co-authors.

Competing Interests

340 The authors declare that they have no conflict of interest.

Acknowledgements

We would like to thank David Roberts, David Evans, Johann Klages, and Coen Hofstede, for conversations that provided helpful insights in the initial preparation stages of this manuscript, and Tobias Binder for helping with data collection in the 2018 EastGRIP season. We acknowledge the use of software from Open Polar Radar generated with support
345 from the University of Kansas, NASA grants 80NSSC20K1242 and 80NSSC21K0753, and NSF grants OPP-2027615, OPP-2019719, OPP-1739003, IIS-1838230, RISE-2126503, RISE-2127606, and RISE-2126468.

EGRIP is directed and organized by the Centre for Ice and Climate at the Niels Bohr Institute, University of Copenhagen. It is supported by funding agencies and institutions in Denmark (A. P. Møller Foundation, University of Copenhagen), USA (US National Science Foundation, Office of Polar Programs), Germany (Alfred Wegener Institute, Helmholtz Centre for Polar and Marine Research), Japan (National Institute of Polar Research and Arctic Challenge for Sustainability), Norway (University of Bergen and Trond Mohn Foundation), Switzerland (Swiss National Science Foundation), France (French Polar Institute Paul-Emile Victor, Institute for Geosciences and Environmental research), Canada (University of Manitoba) and China (Chinese Academy of Sciences and Beijing Normal University).

Financial support

CMC was funded by the Alfred Wegener Institute's INSPIRES III programme.

References

Al-Ibadi, M., Sprick, J., Athinarapu, S., Stumpf, T., Paden, J., Leuschen, C. J., Rodriguez, F., Xu, M., Crandall, D., Fox, G., Burgess, D., Sharp, M., Copland, L., and Van Wychen, W.: DEM extraction of the basal topography of the Canadian Archipelago Ice Caps via 2D automated layer-tracker, IGARSS, 10.1109/IGARSS.2017.8127114, 2017.

Alley, R. B., Holschuh, N., MacAyeal, D. R., Parizek, B. R., Zoet, L., Riverman, K., Muto, A., Christianson, K., Clyne, E., Anandakrishnan, S., Stevens, N., Smith, A., Arthern, R., Bingham, R., Brisbourne, A., Eisen, O., Hofstede, C., Kulessa, B., Sterns, L., Winberry, P., Bodart, J., Borthwick, L., Case, E., Gustafson, C., Kingslake, J., Ockenden, H., Schoonman, C., and Schwans, E.: Bedforms of Thwaites Glacier, West Antarctica: Character and Origin, Journal of Geophysical Research: Earth Surface, 126, 10.1029/2021JF006339, 2021.

Anderson, J. B. and Fretwell, L. O.: Geomorphology of the onset area of a paleo-ice stream, Marguerite Bay, Antarctic Peninsula, Earth Surface Processes and Landforms, 33, 503-512, 10.1002/esp.1662, 2008.

Aschwanden, A., Fahnestock, M. A., and Truffer, M.: Complex Greenland outlet glacier flow captured, Nature Communications, 7, 10.1038/ncomms10524, 2016.

Barchyn, T. E., Dowling, T. P. F., Stokes, C. R., and Hugenholtz, C. H.: Subglacial bed form morphology controlled by ice speed and sediment thickness, Geophysical Research Letters, 43, 7572-7580, 10.1002/2016gl069558, 2016.

Bingham, R. G., Vaughan, D. G., King, E. C., Davies, D., Cornford, S. L., Smith, A. M., Arthern, R. J., Brisbourne, A. M., De Rydt, J., Graham, A. G. C., Spagnolo, M., Marsh, O. J., and Shean, D. E.: Diverse landscapes beneath Pine Island Glacier influence ice flow, Nature Communications, 8, 10.1038/s41467-017-01597-y, 2017.

Bons, P. D., de Riese, T., Franke, S., Llorens, M.-G., Sachau, T., Stoll, N., Weikusat, I., Westhoff, J., and Zhang, Y.: Comment on "Exceptionally high heat flux needed to sustain the Northeast Greenland Ice Stream" by Smith-Johnsen et al. (2020), The Cryosphere, 15, 2251-2254, 10.5194/tc-15-2251-2021, 2021.

Bons, P. D., Jansen, D., Mundel, F., Bauer, C. C., Binder, T., Eisen, O., Jessell, M. W., Llorens, M. G., Steinbach, F., Steinhage, D., and Weikusat, I.: Converging flow and anisotropy cause large-scale folding in Greenland's ice sheet, Nature Communications, 7, 10.1038/ncomms11427, 2016.

380   Canals, M., Urgeles, R., and Calafat, A. M.: Deep sea-floor evidence of past ice streams off the Antarctic Peninsula., Geology, 28, 31-34, doi.org/10.1130/0091-7613(2000)028%3C0031:DSEOPI%3E2.0.CO;2, 2000.

Chandler, B. M. P., Lovell, H., Boston, C. M., Lukas, S., Barr, I. D., Benediktsson, Í. Ö., Benn, D. I., Clark, C. D., Darvill, C. M., Evans, D. J. A., Ewertowski, M., Loibl, D., Margold, M., Otto, J.-C., Roberts, D. H., Stokes, C. R., Storrar, R. D., and Stroeven, A. P.: Glacial geomorphological mapping: a review of approaches and frameworks for best practice, Earth-Science

385   Reviews, 806-846, 10.1016/j.earscirev.2018.07.015, 2018.

Christianson, K., Peters, L. E., Alley, R. B., Anandakrishnan, S., Jacobel, R. W., Riverman, K. L., Muto, A., and Keisling, B. A.: Dilatant till facilitates ice-stream flow in northeast Greenland, Earth and Planetary Science Letters, 401, 57-69, 10.1016/J.EPSL.2014.05.060, 2014.

Chu, W., Schroeder, D. M., Seroussi, H., Creyts, T. T., and Bell, R. E.: Complex Basal Thermal Transition Near the Onset of

390   Petermann Glacier, Greenland, Journal of Geophysical Research: Earth Surface, 123, 985-995, 10.1029/2017jf004561, 2018.

Clark, C. D.: Mega-scale glacial lineations and cross-cutting ice-flow landforms, Earth Surface Processes and Landforms, 18, 1-29, 10.1002/esp.3290180102, 1993.

De Angelis, H. and Kleman, J.: Palaeo-ice-stream onsets: examples from the north-eastern Laurentide Ice Sheet, Earth Surface Processes and Landforms, 33, 560-572, 10.1002/esp.1663, 2008.

395   Dowdeswell, E. K., Todd, B. J., and Dowdeswell, J. A.: Crag-and-tail features: convergent ice flow through Eclipse Sound, Baffin Island, Arctic Canada, in: Atlas of Submarine Glacial Landforms: Modern, Quaternary and Ancient edited by: Dowdeswell, J. A., Canals, M., Jakobsson, M., Todd, B. J., Dowdeswell, E. K., and Hogan, K. A., Geological Society, London, 2016.

Dowdeswell, J. A., Hogan, K. A., Evans, J., Noormets, R., Ó Cofaigh, C., and Ottesen, D.: Past ice-sheet flow east of Svalbard

400   inferred from streamlined subglacial landforms, Geology, 38, 163-166, 10.1130/g30621.1, 2010.

Dowdeswell, J. A., Hogan, K. A., Ó Cofaigh, C., Fugelli, E. M. G., Evans, J., and Noormets, R.: Late Quaternary ice flow in a West Greenland fjord and cross-shelf trough system: submarine landforms from Rink Isbrae to Uummannaq shelf and slope, Quaternary Science Reviews, 92, 292-309, 10.1016/j.quascirev.2013.09.007, 2014.

Ely, J. C., Stevens, D., Clark, C. D., and Butcher, F. E. G.: Numerical modelling of subglacial ribs, drumlins, herringbones,

405   and mega-scale glacial lineations reveals their developmental trajectories and transitions, Earth Surface Processes and Landforms, 10.1002/esp.5529, 2022.

Ely, J. C., Clark, C. D., Spagnolo, M., Stokes, C. R., Greenwood, S. L., Hughes, A. L. C., Dunlop, P., and Hess, D.: Do subglacial bedforms comprise a size and shape continuum?, Geomorphology, 257, 108-119, 10.1016/j.geomorph.2016.01.001, 2016.

410   Eyles, N. and Doughty, M.: Glacially-streamlined hard and soft beds of the paleo- Ontario ice stream in Southern Ontario and New York state, Sedimentary Geology, 338, 51-71, 10.1016/j.sedgeo.2016.01.019, 2016.

Eyles, N., Putkinen, N., Sookhan, S., and Arbelaez-Moreno, L.: Erosional origin of drumlins and megaridges, Sedimentary Geology, 338, 2-23, 10.1016/j.sedgeo.2016.01.006, 2016.

Fahnestock, M., Abdalati, W., Joughin, I., Brozena, J., and Gogineni, P.: High geothermal heat flow, basal melt, and the origin
415   of rapid ice flow in central Greenland, Science, 294, 2338-2342, 10.1126/science.1065370, 2001.

Franke, S., Jansen, D., Binder, T., Dörr, N., Helm, V., Paden, J., Steinhage, D., and Eisen, O.: Bed topography and subglacial landforms in the onset region of the Northeast Greenland Ice Stream, Annals of Glaciology, 61, 143-153, 10.1017/aog.2020.12, 2020.

Franke, S., Bons, P. D., Westhoff, J., Weikusat, I., Binder, T., Streng, K., Steinhage, D., Helm, V., Eisen, O., Paden, J. D.,
420   Eagles, G., and Jansen, D.: Holocene ice-stream shutdown and drainage basin reconfiguration in northeast Greenland, Nature Geoscience, 1-7, 10.1038/s41561-022-01082-2, 2022a.

Franke, S., Jansen, D., Binder, T., Paden, J. D., Dörr, N., Gerber, T. A., Miller, H., Dahl-Jensen, D., Helm, V., Steinhage, D., Weikusat, I., Wilhelms, F., and Eisen, O.: Airborne ultra-wideband radar sounding over the shear margins and along flow lines at the onset region of the Northeast Greenland Ice Stream, Earth System Science Data, 14, 763-779, 10.5194/essd-14-763-
425   2022, 2022b.

Gardner, A., Fahnestock, M., and Scambos, T. A.: MEaSUREs ITS_LIVE Regional Glacier and Ice Sheet Surface Velocities (1), NASA National Snow and Ice Data Center Distributed Active Archive Center [dataset], https://doi.org/10.5067/6II6VW8LLWJ7, 2022.

Gerber, T. A., Lilien, D. A., Rathmann, N. M., Franke, S., Young, T. J., Valero-Delgado, F., Ershadi, M. R., Drews, R., Zeising,
430   O., Humbert, A., Stoll, N., Weikusat, I., Grinsted, A., Hvidberg, C. S., Jansen, D., Miller, H., Helm, V., Steinhage, D., O'Neill, C., Paden, J., Gogineni, S. P., Dahl-Jensen, D., and Eisen, O.: Crystal orientation fabric anisotropy causes directional hardening of the Northeast Greenland Ice Stream, Nat Commun, 14, 2653, 10.1038/s41467-023-38139-8, 2023.

Graham, A. G. C., Larter, R. D., Gohl, K., Hillenbrand, C. D., Smith, J. A., and Kuhn, G.: Bedform signature of a West Antarctic palaeo-ice stream reveals a multi-temporal record of flow and substrate control, Quaternary Science Reviews, 28,
435   2774-2793, 10.1016/J.QUASCIREV.2009.07.003, 2009.

Gudmundsson, G. H. and Jenkins, A.: Ice-flow velocities on Rutford Ice Stream, West Antarctica, are stable over decadal timescales, Journal of Glaciology, 55, 339-344, 10.3189/002214309788608697, 2017.

Hale, R. D., Miller, H., Gogineni, S., Yan, J. B., Rodriguez-Morales, F., Leuschen, C. J., Paden, J. D., Li, J., Binder, T., Steinhage, D., Gehrmann, M., and Braaten, D.: Multi-Channel Ultra-Wideband Radar Sounder and Imager, IGARSS, 2112 -
440   2115, 2016.

Hoffman, A. O., Holschuh, N., Mueller, M., Paden, J., Muto, A., Ariho, G., Brigham, C., Christian, J. E., Davidge, L., Heitmann, E., Hills, B., Horlings, A., Morey, S., O'Connor, G., Fudge, T. J., Steig, E. J., and Christianson, K.: Scars of

tectonism promote ice-sheet nucleation from Hercules Dome into West Antarctica, Nature Geoscience, 1005-1013, 10.1038/s41561-023-01265-5, 2023.

445 Holschuh, N., Lilien, D. A., and Christianson, K.: Thermal Weakening, Convergent Flow, and Vertical Heat Transport in the Northeast Greenland Ice Stream Shear Margins, Geophysical Research Letters, 46, 8184-8193, 10.1029/2019GL083436, 2019.

Holschuh, N., Christianson, K., Paden, J., Alley, R. B., and Anandakrishnan, S.: Linking postglacial landscapes to glacier dynamics using swath radar at Thwaites glacier, Antarctica, Geology, 48, 268-272, 10.1130/G46772.1, 2020.

Hvidberg, C. S., Grinsted, A., Dahl-Jensen, D., Khan, S. A., Kusk, A., Andersen, J. K., Neckel, N., Solgaard, A., Karlsson, N.

450 B., Kjar, H. A., and Vallelonga, P.: Surface velocity of the Northeast Greenland Ice Stream (NEGIS): Assessment of interior velocities derived from satellite data by GPS, Cryosphere, 14, 3487-3502, 10.5194/tc-14-3487-2020, 2020.

Jamieson, S. S. R., Stokes, C. R., Livingstone, S. J., Vieli, A., Ó Cofaigh, C., Hillenbrand, C.-D., and Spagnolo, M.: Subglacial processes on an Antarctic ice stream bed. 2: Can modelled ice dynamics explain the morphology of mega-scale glacial lineations?, Journal of Glaciology, 62, 285-298, 10.1017/jog.2016.19, 2016.

455 Jansen, D., Franke, S., Bauer, C. C., Binder, T., Dahl-Jensen, D., Eichler, J., Eisen, O., Hu, Y., Kerch, J., Llorens, M. G., Miller, H., Neckel, N., Paden, J., de Riese, T., Sachau, T., Stoll, N., Weikusat, I., Wilhelms, F., Zhang, Y., and Bons, P. D.: Shear margins in upper half of Northeast Greenland Ice Stream were established two millennia ago, Nat Commun, 15, 1193, 10.1038/s41467-024-45021-8, 2024.

Jezek, K., Wu, X., Gogineni, P., Rodríguez, E., Freeman, A., Rodriguez-Morales, F., and Clark, C. D.: Radar images of the

460 bed of the Greenland Ice Sheet, Geophysical Research Letters, 38, n/a-n/a, 10.1029/2010gl045519, 2011.

Joughin, I., Smith, B. E., and Howat, I. M.: A complete map of Greenland ice velocity derived from satellite data collected over 20 years, Journal of Glaciology, 64, 1-11, 10.1017/JOG.2017.73, 2018.

Kehew, A. E., Piotrowski, J. A., and Jørgensen, F.: Tunnel valleys: Concepts and controversies — A review, Earth-Science Reviews, 113, 33-58, 10.1016/j.earscirev.2012.02.002, 2012.

465 King, E. C., Hindmarsh, R. C. A., and Stokes, C. R.: Formation of mega-scale glacial lineations observed beneath a West Antarctic ice stream, Nature Geoscience, 2, 585-588, 10.1038/ngeo581, 2009.

King, E. C., Pritchard, H. D., and Smith, A. M.: Subglacial landforms beneath Rutford Ice Stream, Antarctica: detailed bed topography from ice-penetrating radar, Earth System Science Data, 8, 151-158, 10.5194/essd-8-151-2016, 2016.

King, E. C., Woodward, J., and Smith, A. M.: Seismic and radar observations of subglacial bed forms beneath the onset zone

470 of Rutford Ice Stream, Antarctica, Journal of Glaciology, 53, 665-672, 10.3189/002214307784409216, 2007.

Krieger, L., Floricioiu, D., and Neckel, N.: Drainage basin delineation for outlet glaciers of Northeast Greenland based on Sentinel-1 ice velocities and TanDEM-X elevations, Remote Sensing of Environment, 237, 10.1016/j.rse.2019.111483, 2019.

Law, R., Christoffersen, P., MacKie, E., Cook, S., Haseloff, M., and Gagliardini, O.: Complex motion of Greenland Ice Sheet outlet glaciers with basal temperate ice, Science Advances, 9, eabq5180, 2023.

475 Livingstone, S. J. and Clark, C. D.: Morphological properties of tunnel valleys of the southern sector of the Laurentide Ice Sheet and implications for their formation, Earth Surface Dynamics, 4, 567-589, 10.5194/esurf-4-567-2016, 2016.

Margold, M., Stokes, C. R., and Clark, C. D.: Ice streams in the Laurentide Ice Sheet: Identification, characteristics and comparison to modern ice sheets, Earth-Science Reviews, 143, 117-146, 10.1016/j.earscirev.2015.01.011, 2015.

Morlighem, M., Williams, C., Rignot, E., An, L., Arndt, J. E., Bamber, J. L., Catania, G., Chauche, N., Dowdeswell, J. A.,
480   Dorschel, B., Fenty, I., Hogan, K., Howat, I., Hubbard, A. L., Jakobsson, M., Jordan, T. M., Kjeldsen, K. K., Millan, R., Mayer, L., Mouginot, J., Noel, B. P. Y., O'Cofaigh, C., Palmer, S. J., Rysgaard, S., Seroussi, H., Siegert, M. J., Slabon, P., Straneo, F., van den Broeke, M. R., Weinrebe, W., Wood, M., and Zinglersen, K. B.: IceBridge BedMachine Greenland, Version 5, NASA National Snow and Ice Data Center Distributed Active Archive Center [dataset], https://doi.org/10.5067/GMEVBWFLWA7X, 2022.

485   Morlighem, M., Williams, C. N., Rignot, E., An, L., Arndt, J. E., Bamber, J. L., Catania, G., Chauche, N., Dowdeswell, J. A., Dorschel, B., Fenty, I., Hogan, K., Howat, I., Hubbard, A., Jakobsson, M., Jordan, T. M., Kjeldsen, K. K., Millan, R., Mayer, L., Mouginot, J., Noel, B. P. Y., O'Cofaigh, C., Palmer, S., Rysgaard, S., Seroussi, H., Siegert, M. J., Slabon, P., Straneo, F., van den Broeke, M. R., Weinrebe, W., Wood, M., and Zinglersen, K. B.: BedMachine v3: Complete Bed Topography and Ocean Bathymetry Mapping of Greenland From Multibeam Echo Sounding Combined With Mass Conservation, Geophys Res
490   Lett, 44, 11051-11061, 10.1002/2017GL074954, 2017.

Mouginot, J., Rignot, E., Bjork, A. A., van den Broeke, M., Millan, R., Morlighem, M., Noel, B., Scheuchl, B., and Wood, M.: Forty-six years of Greenland Ice Sheet mass balance from 1972 to 2018, Proc Natl Acad Sci U S A, 116, 9239-9244, 10.1073/pnas.1904242116, 2019.

Mulligan, R. P. M., Eyles, C. H., and Marich, A. S.: Subglacial and ice-marginal landforms in south-central Ontario:
495   implications for ice-sheet reconfiguration during deglaciation, Boreas, 48, 635-657, 10.1111/bor.12372, 2019.

Newton, M., Evans, D. J. A., Roberts, D. H., and Stokes, C. R.: Bedrock mega-grooves in glaciated terrain: A review, Earth-Science Reviews, 185, 57-79, 10.1016/j.earscirev.2018.03.007, 2018.

Newton, M., Stokes, C. R., Roberts, D. H., and Evans, D. J. A.: Characteristics and formation of bedrock mega-grooves (BMGs) in glaciated terrain: 1 - morphometric analyses, Geomorphology, 427, 10.1016/j.geomorph.2023.108619, 2023.

500   Nitsche, F. O., Larter, R. D., Gohl, K., Graham, A. G. C., and Kuhn, G.: Crag-and-tail features on the Amundsen Sea continental shelf, West Antarctica, in: Atlas of Submarine Glacial Landforms: Modern, Quaternary and Ancient, edited by: Dowdeswell, J. A., Canals, M., Jakobsson, M., Todd, B. J., Dowdeswell, E. K., and Hogan, K., Geological Society, London, 2016.

Otosaka, I. N., Shepherd, A., Ivins, E. R., Schlegel, N.-J., Amory, C., van den Broeke, M. R., Horwath, M., Joughin, I., King,
505   M. D., Krinner, G., Nowicki, S., Payne, A. J., Rignot, E., Scambos, T., Simon, K. M., Smith, B. E., Sørensen, L. S., Velicogna, I., Whitehouse, P. L., A, G., Agosta, C., Ahlstrøm, A. P., Blazquez, A., Colgan, W., Engdahl, M. E., Fettweis, X., Forsberg, R., Gallée, H., Gardner, A., Gilbert, L., Gourmelen, N., Groh, A., Gunter, B. C., Harig, C., Helm, V., Khan, S. A., Kittel, C., Konrad, H., Langen, P. L., Lecavalier, B. S., Liang, C.-C., Loomis, B. D., McMillan, M., Melini, D., Mernild, S. H., Mottram, R., Mouginot, J., Nilsson, J., Noël, B., Pattle, M. E., Peltier, W. R., Pie, N., Roca, M., Sasgen, I., Save, H. V., Seo, K.-W.,
510   Scheuchl, B., Schrama, E. J. O., Schröder, L., Simonsen, S. B., Slater, T., Spada, G., Sutterley, T. C., Vishwakarma, B. D.,

van Wessem, J. M., Wiese, D., van der Wal, W., and Wouters, B.: Mass balance of the Greenland and Antarctic ice sheets from 1992 to 2020, Earth System Science Data, 15, 1597-1616, 10.5194/essd-15-1597-2023, 2023.

Paden, J., Akins, T., Dunson, D., Allen, C., and Gogineni, P.: Ice-sheet bed 3-D tomography, Journal of Glaciology, 56, 3-11, 10.3189/002214310791190811, 2010.

515 Paden, J. D., Mathews, R., jiluli, mohanadalibadi, theresea-moore, da Silva, V. B., jsprick, Talasila, H. M., Gordon, Holschuh, N., gamer10bm, Barnett, C., Aegidius7, Chu, S., Ibikunle, Jutila, A., Choudhari, R., and Christoffersen, M.: Open Polar Radar (3.01) [code], https://doi.org/10.5281/zenodo.5683959, 2023.

QGIS.org: QGIS Geographic Information System. Open Source Geospatial Foundation Project. http://qgis.org [code], 2025.

Rathmann, N. M. and Lilien, D. A.: Inferred basal friction and mass flux affected by crystal-orientation fabrics, Journal of

520 Glaciology, 68, 236-252, 10.1017/JOG.2021.88, 2022.

Riverman, K. L., Anandakrishnan, S., Alley, R. B., Holschuh, N., Dow, C. F., Muto, A., Parizek, B. R., Christianson, K., and Peters, L. E.: Wet subglacial bedforms of the NE Greenland Ice Stream shear margins, Annals of Glaciology, 60, 91-99, 10.1017/aog.2019.43, 2019.

Roberts, D. H., Grimoldi, E., Callard, L., Evans, D. J. A., Clark, C. D., Stewart, H. A., Dove, D., Saher, M., Ó Cofaigh, C.,

525 Chiverrell, R. C., Bateman, M. D., Moreton, S. G., Bradwell, T., Fabel, D., and Medialdea, A.: The mixed-bed glacial landform imprint of the North Sea Lobe in the western North Sea, Earth Surface Processes and Landforms, 44, 1233-1258, 10.1002/esp.4569, 2019.

Rysgaard, S., Bendtsen, J., Mortensen, J., and Sejr, M. K.: High geothermal heat flux in close proximity to the Northeast Greenland Ice Stream, Scientific Reports, 8, 10.1038/s41598-018-19244-x, 2018.

530 Schlegel, R., Murray, T., Smith, A. M., Brisbourne, A. M., Booth, A. D., King, E. C., and Clark, R. A.: Radar Derived Subglacial Properties and Landforms Beneath Rutford Ice Stream, West Antarctica, Journal of Geophysical Research: Earth Surface, 127, 10.1029/2021jf006349, 2022.

Shepherd, A., Ivins, E., Rignot, E., Smith, B., van den Broeke, M., Velicogna, I., Whitehouse, P., Briggs, K., Joughin, I., Krinner, G., Nowicki, S., Payne, T., Scambos, T., Schlegel, N., A, G., Agosta, C., Ahlstrøm, A., Babonis, G., Barletta, V. R.,

535 Bjørk, A. A., Blazquez, A., Bonin, J., Colgan, W., Csatho, B., Cullather, R., Engdahl, M. E., Felikson, D., Fettweis, X., Forsberg, R., Hogg, A. E., Gallee, H., Gardner, A., Gilbert, L., Gourmelen, N., Groh, A., Gunter, B., Hanna, E., Harig, C., Helm, V., Horvath, A., Horwath, M., Khan, S., Kjeldsen, K. K., Konrad, H., Langen, P. L., Lecavalier, B., Loomis, B., Luthcke, S., McMillan, M., Melini, D., Mernild, S., Mohajerani, Y., Moore, P., Mottram, R., Mouginot, J., Moyano, G., Muir, A., Nagler, T., Nield, G., Nilsson, J., Noël, B., Otosaka, I., Pattle, M. E., Peltier, W. R., Pie, N., Rietbroek, R., Rott, H.,

540 Sandberg Sørensen, L., Sasgen, I., Save, H., Scheuchl, B., Schrama, E., Schröder, L., Seo, K.-W., Simonsen, S. B., Slater, T., Spada, G., Sutterley, T., Talpe, M., Tarasov, L., van de Berg, W. J., van der Wal, W., van Wessem, M., Vishwakarma, B. D., Wiese, D., Wilton, D., Wagner, T., Wouters, B., Wuite, J., and The, I. T.: Mass balance of the Greenland Ice Sheet from 1992 to 2018, Nature, 579, 233-239, 10.1038/s41586-019-1855-2, 2020.

Smith-Johnsen, S., de Fleurian, B., Schlegel, N., Seroussi, H., and Nisanciolgu, K.: Exceptionally High Geothermal Heat Flux
545 Needed to Sustain the Northeast Greenland Ice Stream, The Cryosphere, 841-854, 10.5194/tc-14-841-2020, 2020.

Spagnolo, M., Clark, C. D., Ely, J. C., Stokes, C. R., Anderson, J. B., Andreassen, K., Graham, A. G. C., and King, E. C.: Size, shape and spatial arrangement of mega-scale glacial lineations from a large and diverse dataset, Earth Surface Processes and Landforms, 39, 1432-1448, 10.1002/esp.3532, 2014.

Stokes, C. R.: Geomorphology under ice streams: Moving from form to process, Earth Surface Processes and Landforms, 43,
550 85-123, 10.1002/esp.4259, 2018.

Stokes, C. R. and Clark, C. D.: Are long subglacial bedforms indicative of fast ice flow?, Boreas, 31, 239-249, 10.1111/J.1502-3885.2002.TB01070.X, 2002a.

Stokes, C. R. and Clark, C. D.: Ice stream shear margin moraines, Earth Surface Processes and Landforms, 27, 547-558, 10.1002/ESP.326, 2002b.

555 Stokes, C. R., Spagnolo, M., Clark, C. D., Ó Cofaigh, C., Lian, O. B., and Dunstone, R. B.: Formation of mega-scale glacial lineations on the Dubawnt Lake Ice Stream bed: 1. size, shape and spacing from a large remote sensing dataset, Quaternary Science Reviews, 77, 190-209, 10.1016/J.QUASCIREV.2013.06.003, 2013.

Stokes, C. R., Tarasov, L., Blomdin, R., Cronin, T. M., Fisher, T. G., Gyllencreutz, R., Hättestrand, C., Heyman, J., Hindmarsh, R. C. A., Hughes, A. L. C., Jakobsson, M., Kirchner, N., Livingstone, S. J., Margold, M., Murton, J. B., Noormets, R., Peltier,
560 W. R., Peteet, D. M., Piper, D. J. W., Preusser, F., Renssen, H., Roberts, D. H., Roche, D. M., Saint-Ange, F., Stroeven, A. P., and Teller, J. T.: On the reconstruction of palaeo-ice sheets: Recent advances and future challenges, Quaternary Science Reviews, 125, 15-49, 10.1016/j.quascirev.2015.07.016, 2015.

Stoll, N., Weikusat, I., Jansen, D., Bons, P., Darányi, K., Westhoff, J., Llorens, M.-G., Wallis, D., Eichler, J., Saruya, T., Homma, T., Drury, M., Wilhelms, F., Kipfstuhl, S., Dahl-Jensen, D., and Kerch, J.: EastGRIP ice core reveals the exceptional
565 evolution of crystallographic preferred orientation throughout the Northeast Greenland Ice Stream, 10.5194/egusphere-2024-2653, 2024.

Tabone, I., Robinson, A., Montoya, M., and Alvarez-Solas, J.: Holocene thinning in central Greenland controlled by the Northeast Greenland Ice Stream, Nat Commun, 15, 6434, 10.1038/s41467-024-50772-5, 2024.

Vérité, J., Ravier, É., Bourgeois, O., Bessin, P., and Pochat, S.: New metrics reveal the evolutionary continuum behind the
570 morphological diversity of subglacial bedforms, Geomorphology, 427, 10.1016/j.geomorph.2023.108627, 2023.

Woodward, J. and King, E. C.: Radar surveys of the Rutford Ice Stream onset zone, West Antarctica: indications of flow (in)stability?, Annals of Glaciology, 50, 57-62, 10.3189/172756409789097469, 2009.

Zoet, L. K., Rawling, J. E., Woodard, J. B., Barrette, N., and Mickelson, D. M.: Factors that contribute to the elongation of drumlins beneath the Green Bay Lobe, Laurentide Ice Sheet, Earth Surface Processes and Landforms, 46, 2540-2550,
575 10.1002/esp.5192, 2021.